



HAL
open science

Markovian approximation of the rough Bergomi model for Monte Carlo option pricing

Qinwen Zhu, Gregoire Loeper, Wen Chen, Nicolas Langrené

► **To cite this version:**

Qinwen Zhu, Gregoire Loeper, Wen Chen, Nicolas Langrené. Markovian approximation of the rough Bergomi model for Monte Carlo option pricing. *Mathematics*, 2021, 9 (5), pp.528. 10.3390/math9050528. hal-02910724v2

HAL Id: hal-02910724

<https://hal.science/hal-02910724v2>

Submitted on 13 Apr 2022

HAL is a multi-disciplinary open access archive for the deposit and dissemination of scientific research documents, whether they are published or not. The documents may come from teaching and research institutions in France or abroad, or from public or private research centers.

L'archive ouverte pluridisciplinaire **HAL**, est destinée au dépôt et à la diffusion de documents scientifiques de niveau recherche, publiés ou non, émanant des établissements d'enseignement et de recherche français ou étrangers, des laboratoires publics ou privés.

Article

Markovian Approximation of the Rough Bergomi Model for Monte Carlo Option Pricing

Qinwen Zhu ¹, Grégoire Loeper ², Wen Chen ³ and Nicolas Langrené ^{3,*} 

¹ School of Mathematical Sciences, Nanjing Normal University, Nanjing 210023, China; qinwen.wendy.zhu@gmail.com

² School of Mathematics & Centre for Quantitative Finance and Investment Strategies, Monash University, Clayton, VIC 3800, Australia; gregoire.loeper@monash.edu

³ Data61, Commonwealth Scientific and Industrial Research Organisation, Melbourne, VIC 3008, Australia; wen.chen@csiro.au

* Correspondence: nicolas.langrene@csiro.au

Abstract: The recently developed rough Bergomi (rBergomi) model is a rough fractional stochastic volatility (RFSV) model which can generate a more realistic term structure of at-the-money volatility skews compared with other RFSV models. However, its non-Markovianity brings mathematical and computational challenges for model calibration and simulation. To overcome these difficulties, we show that the rBergomi model can be well-approximated by the forward-variance Bergomi model with wisely chosen weights and mean-reversion speed parameters (aBergomi), which has the Markovian property. We establish an explicit bound on the L2-error between the respective kernels of these two models, which is explicitly controlled by the number of terms in the aBergomi model. We establish and describe the affine structure of the rBergomi model, and show the convergence of the affine structure of the aBergomi model to the one of the rBergomi model. We demonstrate the efficiency and accuracy of our method by implementing a classical Markovian Monte Carlo simulation scheme for the aBergomi model, which we compare to the hybrid scheme of the rBergomi model.

Keywords: rough fractional stochastic volatility; forward variance model; markovian representation; volatility skew; Volterra integral; rough heston; hybrid scheme; sum of ornstein-uhlenbeck processes



Citation: Zhu, Q.; Loeper, G.; Chen, W.; Langrené, N. Markovian Approximation of the Rough Bergomi Model for Monte Carlo Option Pricing. *Mathematics* **2021**, *9*, 528. <https://doi.org/10.3390/math9050528>

Academic Editors: Elisa Alòs and Jorge A. León

Received: 17 December 2020
Accepted: 25 February 2021
Published: 3 March 2021

Publisher's Note: MDPI stays neutral with regard to jurisdictional claims in published maps and institutional affiliations.



Copyright: © 2021 by the authors. Licensee MDPI, Basel, Switzerland. This article is an open access article distributed under the terms and conditions of the Creative Commons Attribution (CC BY) license (<https://creativecommons.org/licenses/by/4.0/>).

1. Introduction

The rough Bergomi (rBergomi) model introduced by Bayer et al. [1] has gained acceptance for stochastic volatility modelling due to its power-law at-the-money (ATM) volatility skew, which is consistent with empirical studies (see Forde and Zhang [2], Fukasawa [3], Gatheral et al. [4]) and with the effect of the no-arbitrage assumption on the market impact function (see Jusselin and Rosenbaum [5]). However, the stochastic process which characterizes this volatility model is rougher than that of a Brownian motion; in particular, the lack of Markovianity makes classical pricing methods infeasible.

In order to price options under an rBergomi model, Bayer et al. [6] proposed hierarchical adaptive sparse grids, Jacquier et al. [7] developed pricing algorithms for VIX futures and options, and McCrickerd and Pakkanen [8] developed a “turbocharged” Monte Carlo pricing method. A number of short-term approximations have been proposed to obtain fast approximations for short maturities—see, for example, Fukasawa [3], El Euch et al. [9], Bayer et al. [10], and Friz et al. [11]. Regarding the pricing of exotic options in the rBergomi model, Tomas [12] considered the pricing of Asian options, and Bayer et al. [13] and Bayer et al. [14] considered the pricing of American put options. Besides pricing, the calibration of the rBergomi model is also a challenge, for which Bayer et al. [15], Zeron and Ruiz [16], and Horvath et al. [17] propose to use deep learning methods. In spite of this number of recent efforts, the inherent challenges brought by the rBergomi model still prevent its widespread adoption in the industry.

Inspired by the technique by Abi Jaber and El Euch [18], Gatheral and Keller-Ressel [19], and Harms and Stefanovits [20], in which the authors designed a multi-factor stochastic volatility model with Markovian structure to approximate the rough Heston model, we establish an analogous multi-factor affine structure for the rBergomi model. Indeed, the Volterra kernel of the rBergomi model corresponds to a superposition of infinitely many Ornstein-Uhlenbeck (OU) processes with different speeds of mean reversion. Truncating this infinite sum into a finite sum of OU processes yields an approximation of the rBergomi model which is a classical Markovian multi-factor Bergomi model. We refer to this affine, Markovian approximation of the rBergomi model as the aBergomi model. We prove the existence and uniqueness of the solution to this aBergomi model, and show that its affine structure converges to the one of the rBergomi model. Finally, we implement a Monte Carlo scheme for the aBergomi model, and compare it to the hybrid scheme of the rBergomi model (Bennedsen et al. [21]). Our numerical tests demonstrate that using 20 exponential terms in the aBergomi kernel is sufficient to obtain accurate implied volatility curvatures while remaining computationally efficient.

The idea to interpret the conventional two-factor Bergomi model as a Markovian approximation of the rBergomi model was originally briefly suggested by Bayer et al. [1] (p. 892). Our work explores and expands upon this intuition by testing the number of factors to use in the Bergomi model and establishing their respective parameters for best approximation of the rBergomi model. For comprehensiveness, one can mention the alternative Markovian approximation proposed in Carr and Itkin [22] of the rough volatility version of the mean-reverting lognormal volatility model of Sepp [23], Langrené et al. [24], based on a closed-form vol-of-vol expansion for solving the pricing PDE arising from the use of the Dobrić-Ojeda process (Dobrić and Ojeda [25]) to approximate the fractional Brownian motion.

Compared to alternative pricing methods for the rBergomi model, the main advantage of our proposed Markovian approximation approach is that it does not require pricing methods specifically designed for rough volatility models; instead, classical Markovian pricing methods can be used for both vanilla and exotic options. In practice, the Monte Carlo pricing method is the method of choice for the aBergomi model in view of the number of terms needed for good accuracy. The computational cost of simulating our proposed aBergomi model is proportional to the number of time-steps N , which makes it an interesting alternative to the approximate $\mathcal{O}(N \log N)$ hybrid scheme of Bennedsen et al. [21] and the exact $\mathcal{O}(N^3)$ covariance-based scheme of Bayer et al. [1], Bayer et al. [10]. The main downside is that the approximation of the rBergomi power kernel by a sum of exponential terms introduces some error, for which we provide an explicit bound in the L^2 sense. In particular, as in the case of the Riemann-sum scheme of Bennedsen et al. [21], the Fourier-based scheme of Benth et al. [26], or the approximation by a Dobrić-Ojeda process in Carr and Itkin [22], a truncation of the power kernel singularity at $s = t$ cannot be avoided.

The paper is organized as follows. In Section 2, we introduce the Bergomi and rBergomi models and discuss their respective ATM volatility skews. The rBergomi model is closely related to the RFSV model introduced in Alòs et al. [27], for which the ATM volatility is proved to be equivalent to the power $T^{H-\frac{1}{2}}$ for short maturity using the Malliavin technique, a result confirmed in Fukasawa [3] using a martingale expansion approach. We prove in this section that a similar result holds for the rBergomi model, while this does not hold for the Bergomi model (Equation (9)). We also establish the quasi-affine structure of the rough Bergomi model. Section 3 is dedicated to the approximation of the rough Bergomi model by a multi-factor Bergomi model, both theoretically and numerically. Finally, Section 4 compares numerical simulations of the rBergomi model with our approximated Bergomi (aBergomi) model with a finite number of terms, showing the effectiveness of our approximation.

2. Rough Bergomi Skew and Quasi-Affine Structure

Firstly, this section introduces the Bergomi and rough Bergomi stochastic volatility models (Definitions 1 and 2), along with the corresponding notations used throughout the paper.

We consider a filtered probability space $(\Omega, \mathcal{F}, (\mathcal{F}_t)_{t \geq 0}, \mathbb{Q})$, which supports two-dimensional correlated Brownian motions W and B . A log price process $X_t := \log(S_t)$ is assumed to follow the dynamics

$$dX_t = -\frac{1}{2}V_t dt + \sqrt{V_t}dW_t, \tag{1}$$

where $V_t \geq 0$ is the instantaneous spot variance process. Let $\zeta_t^u, u \geq t$ be the instantaneous forward variance for date u observed at time t ; in particular, $\zeta_t^t = V_t$ corresponds to the spot variance.

Bayer et al. [1] proposed the so-called rough Bergomi model where the forward variance follows

$$d\zeta_t^u = \zeta_t^u \eta \sqrt{2\alpha + 1}(u - t)^\alpha dB_t, \quad u \geq t, \tag{2}$$

where W and B have correlation ρ , $\alpha \triangleq H - \frac{1}{2} \in (-\frac{1}{2}, 0)$ is a negative exponent depending on the Hurst exponent $H \in (0, \frac{1}{2})$ of the underlying fractional Brownian motion, and η is a positive parameter depending on H . The definition of the rBergomi model is summarized below:

Definition 1. *The rBergomi stochastic volatility model takes the form*

$$\begin{cases} dX_t = -\frac{1}{2}V_t dt + \sqrt{V_t}dW_t, \\ d\zeta_t^u = \zeta_t^u \eta \sqrt{2\alpha + 1}(u - t)^\alpha dB_t, \end{cases} \tag{3}$$

where $\alpha = H - \frac{1}{2} \in (-\frac{1}{2}, 0)$, and $d\langle W, B \rangle_t = \rho dt$.

By contrast, the two-factor Bergomi model is defined as follows.

Definition 2. *The two-factor Bergomi model (Bergomi [28], Bergomi [29]) is defined by:*

$$\begin{cases} dX_t = -\frac{1}{2}V_t dt + \sqrt{V_t}dW_t^S, \\ d\zeta_t^u = \zeta_t^u \alpha_\theta \omega \left((1 - \theta)e^{-\kappa_X(u-t)} dW_t^X + \theta e^{-\kappa_Y(u-t)} dW_t^Y \right), \end{cases} \tag{4}$$

with

$$\begin{aligned} d\langle W^S, W^X \rangle_t &= \rho_{SX} dt, \\ d\langle W^S, W^Y \rangle_t &= \rho_{SY} dt, \\ d\langle W^X, W^Y \rangle_t &= \rho_{XY} dt, \end{aligned}$$

where $\zeta_t^t = V_t = \omega$ is the lognormal volatility of the instantaneous variance under the normalizing factor $\alpha_\theta = ((1 - \theta)^2 + 2\rho_{XY}\theta(1 - \theta) + \theta^2)^{-\frac{1}{2}}$ and θ is a mixing parameter of the short-term factor driven by W^X and the long-term factor driven by W^Y ($\kappa_X > \kappa_Y$).

Assumption 1. *Without loss of generality, we assume throughout the paper that the initial forward variance curve $\zeta_0^u, u \geq 0$ is flat. This simplification is common in the rBergomi literature; see, for example, Bayer et al. [1], Bayer et al. [6], and Bayer et al. [15]. We henceforth use the notation ζ_0 for the constant initial forward variance curve.*

2.1. ATM Volatility Skew

This subsection derives the ATM volatility skew of the rBergomi and Bergomi models, as the more realistic ATM volatility skew of the rBergomi model over the one of the Bergomi model is one of the motivations behind the introduction of the rBergomi model.

From Bergomi and Guyon [30], we can define the price and the volatility dynamics of a generic stochastic volatility model as follows:

$$\begin{cases} dX_t = -\frac{1}{2}V_t dt + \sqrt{V_t}dW_t, \\ d\zeta_t^u = \lambda(t, u, \zeta_t^u)dB_t, \end{cases} \tag{5}$$

where $X_t = \ln(S_t)$ is the log-spot, V_t is the instantaneous spot variance, ζ_t^u is the instantaneous forward variance for date u observed at time t , and $\lambda = (\lambda_1, \dots, \lambda_d)$ is the volatility of forward instantaneous variances which takes values in \mathbb{R}^d where d is the dimension of the Brownian motion B . Note that in this formulation, the covariance between spot and variance is modelled through the first component of λ , see Bergomi and Guyon [30] for more details.

One can derive the following second-order expression (w.r.t. volatility of volatility) for the Black-Scholes implied volatility:

$$\sigma_{BS}(k, T) = \hat{\sigma}_T^{ATM} + \mathcal{S}_T k + \mathcal{C}_T k^2 + \mathcal{O}(\varepsilon^3), \tag{6}$$

where $k = \ln\left(\frac{K}{S_0}\right)$, K is the strike and ε is a dimensionless scaling factor for the volatility of variances. The ATM volatility and the two coefficients \mathcal{S}_T and \mathcal{C}_T are given by

$$\begin{aligned} \hat{\sigma}_T^{ATM} &= \hat{\sigma}_T^{VS} \left[1 + \frac{\varepsilon}{4v} C^{X\zeta} + \frac{\varepsilon^2}{32v^3} \left(12(C^{X\zeta})^2 - v(v+4)C^{\zeta\zeta} + 4v(v-4)C^\mu \right) \right], \\ \mathcal{S}_T &= \hat{\sigma}_T^{VS} \left[\frac{\varepsilon}{2v^2} C^{X\zeta} + \frac{\varepsilon^2}{8v^3} \left(4C^\mu v - 3(C^{X\zeta})^2 \right) \right], \\ \mathcal{C}_T &= \hat{\sigma}_T^{VS} \frac{\varepsilon^2}{8v^4} \left[4C^\mu v + C^{\zeta\zeta} v - 6(C^{X\zeta})^2 \right], \end{aligned}$$

where $v = \int_0^T \zeta_0^s ds$ is the total variance to expiration T , $\hat{\sigma}_T^{VS} = \sqrt{\frac{v}{T}} = \sqrt{\frac{\int_0^T \zeta_0^s ds}{T}}$ is the effective volatility. Here, $\zeta_0^u = \zeta_0$ for any $u \geq 0$ under Assumption 1, which means that $v = \zeta_0 T$ and $\hat{\sigma}_T^{VS} = \sqrt{\zeta_0}$.

From Bergomi and Guyon [30], we can derive the following second-order expansion for the autocorrelations $C^{X\zeta}$, $C^{\zeta\zeta}$, C^μ :

- $C_t^{X\zeta}(\zeta) = \int_t^T ds \int_s^T du \mu(s, u, \zeta) = \int_t^T ds \int_s^T du \frac{\mathbb{E}[dX_s d\zeta_s^u]}{ds}$ is the doubly integrated spot-variance covariance function,
- $C^{X\zeta} = C_0^{X\zeta}(\zeta_0) = \int_0^T ds \int_s^T du \frac{\mathbb{E}[dX_s d\zeta_0^u]}{ds}$.
- $C_t^{\zeta\zeta}(\zeta) = \int_t^T ds \int_s^T du \int_s^T du' v(s, u, u', \zeta) = \int_t^T ds \int_s^T du \int_s^T u' \frac{\mathbb{E}[d\zeta_s^u d\zeta_s^{u'}]}{ds}$ is the triply integrated variance/variance covariance function,
- $C^{\zeta\zeta} = C_0^{\zeta\zeta}(\zeta_0) = \int_0^T dt \int_s^T du \int_s^T du' \frac{\mathbb{E}[d\zeta_0^u d\zeta_0^{u'}]}{ds}$.
- $C_t^\mu(\zeta) = \int_t^T ds \int_s^T du \mu(s, u, \zeta) \partial_{\zeta_0^u} \left(C_s^{X\zeta}(\zeta) \right)$ is the double time-integral of the instance spot variance covariance function times the sensitivity of $C_t^{X\zeta}(\zeta)$ with respect to instantaneous forward variances,
- $C^\mu = C_0^\mu(\zeta_0) = \int_0^T ds \int_s^T du \frac{\mathbb{E}[dX_s d\zeta_0^u]}{ds} \partial_{\zeta_0^u} \left(C_s^{X\zeta}(\zeta) \right)$,

where μ and ν are given by

$$\begin{aligned} \mu(t, u, y) &= \sqrt{y^t} \lambda_1(t, u, y) = \frac{\mathbb{E}[dX_t d\zeta_t^u | \zeta_t = y]}{dt} = \frac{\mathbb{E}\left[\frac{dS_t}{S_t} d\zeta_t^u | \zeta_t = y\right]}{dt}, \\ \nu(t, u, u', y) &= \sum_{i=1}^d \lambda_i(t, u, y) \lambda_i(t, u', y) = \frac{\mathbb{E}\left[d\zeta_t^u d\zeta_t^{u'} | \zeta_t = y\right]}{dt}. \end{aligned} \tag{7}$$

2.1.1. ATM Volatility Skew in the rBergomi Model

Theorem 1. *In the rBergomi model (3), the ATM volatility skew $\psi(T)$ satisfies*

$$\psi(T) \triangleq \left. \frac{\partial}{\partial k} \sigma_{BS}(k, T) \right|_{k=0} \sim T^{H-\frac{1}{2}}. \tag{8}$$

Proof. We first explicit the autocorrelation functional in the rBergomi model. Using the fact that $\frac{\mathbb{E}[dX_t d\zeta_t^u]}{dt} = \rho\eta\sqrt{2\alpha+1}(u-t)^\alpha \sqrt{\zeta_t^t \zeta_t^u}$, the autocorrelation functionals $C^{X\zeta}$ and $C^{\zeta\zeta}$ are given by

$$\begin{aligned} C^{X\zeta} &= \int_0^T ds \int_s^T du \frac{\mathbb{E}[dX_s d\zeta_0^u]}{ds} \\ &= \rho\eta\sqrt{2\alpha+1} \int_0^T \sqrt{\zeta_0^s} ds \int_s^T \zeta_0^u (u-s)^\alpha du + \mathcal{O}(\varepsilon^3), \\ C^{\zeta\zeta} &= \int_0^T ds \int_s^T du \int_s^T du' \frac{\mathbb{E}[d\zeta_0^u d\zeta_0^{u'}]}{ds} \\ &= \int_0^T ds \int_s^T du \int_s^T du' \eta^2 (2\alpha+1) (u-s)^\alpha (u'-s)^\alpha \zeta_0^u \zeta_0^{u'} \\ &= \eta^2 (2\alpha+1) \int_0^T ds \left(\int_0^T \zeta_0^u (u-s)^\alpha du \right)^2 + \mathcal{O}(\varepsilon^4). \end{aligned}$$

Then, using the fact that

$$\begin{aligned} \partial_{\zeta_s^u} (C_s^{X\zeta}(\zeta)) &= \rho\eta\sqrt{2\alpha+1} \left[\int_s^T dt \sqrt{\zeta_s^t} (u-t)^\alpha \mathbf{1}_{u>t} + \frac{1}{2\sqrt{\zeta_s^u}} \int_u^T \zeta_s^t (t-u)^\alpha dt \right] \\ &= \rho\eta\sqrt{2\alpha+1} \left[\int_s^u dt \sqrt{\zeta_s^t} (u-t)^\alpha + \frac{1}{2\sqrt{\zeta_s^u}} \int_u^T \zeta_s^t (t-u)^\alpha dt \right], \end{aligned}$$

we obtain

$$\begin{aligned} C^\mu &= \int_0^T ds \int_s^T du \frac{\mathbb{E}[dX_s d\zeta_0^u]}{dt} \partial_{\zeta_0^u} (C_s^{X\zeta}(\zeta)) \\ &= \rho^2 \eta^2 (2\alpha+1) \int_0^T \sqrt{\zeta_0^s} ds \int_s^T (u-s)^\alpha du \\ &\quad \times \left[\int_s^u \sqrt{\zeta_0^t} \zeta_0^u (u-t)^\alpha dt + \frac{\sqrt{\zeta_0^u}}{2} \int_u^T \zeta_0^t (t-u)^\alpha dt \right] + \mathcal{O}(\varepsilon^4). \end{aligned}$$

Therefore, using Assumption 1, we obtain the following explicit first-order approximation:

$$C^{X\zeta} = \rho\eta\sqrt{2H} \int_0^T \sqrt{\zeta_0} ds \int_s^T \zeta_0 (u-s)^\alpha du + \mathcal{O}(\varepsilon^3) \approx C_{HP} \rho \zeta_0^{\frac{3}{2}} T^{H+\frac{3}{2}},$$

where C_H is a constant depending on H . We are then able to compute the first-order approximations of the three correlation values $C^{X\xi}$, $C^{\xi\xi}$, C^μ explicitly. The first-order approximation of $\sigma_{BS}(k, T)$ can be written as follows:

$$\begin{aligned} \sigma_{BS}(k, T) &= \hat{\sigma}_T^{VS} + \frac{1}{4v} C^{X\xi} \hat{\sigma}_T^{VS} \varepsilon + \frac{1}{2v^2} C^{X\xi} \hat{\sigma}_T^{VS} \varepsilon k \\ &= \hat{\sigma}_T^{VS} + \left(\frac{1}{4v} + \frac{k}{2v^2} \right) C_H \rho \xi_0^{\frac{3}{2}} T^{H+\frac{3}{2}} \hat{\sigma}_T^{VS} \varepsilon \\ &= \sqrt{\xi_0} + \left(\frac{\xi_0 T}{4} + \frac{k}{2} \right) C_H \rho T^{H-\frac{1}{2}} \varepsilon. \end{aligned}$$

Thus, the ATM volatility skew generated by the rBergomi model satisfies (8), which is consistent with empirical evidence (see for example, Gatheral et al. [4]). □

Remark 1. Besides the rBergomi model, there exist other fractional volatility models which also satisfy Equation (8); see, for example, Fukasawa [31] (subsection 3.3).

2.1.2. ATM Volatility Skew in the Two-Factor Bergomi Model

We now compare this result to the volatility skew in the classical two-factor Bergomi model.

Theorem 2. In the two-factor Bergomi model, the ATM volatility skew satisfies

$$\psi(T) \sim \frac{C_1(\kappa_X T - 1 + e^{-\kappa_X T})}{T^2} + \frac{C_2(\kappa_Y T - 1 + e^{-\kappa_Y T})}{T^2}. \tag{9}$$

Proof. The Brownian motions W^S, W^X, W^Y can be decomposed as:

$$\begin{aligned} W^S &= W^1, \\ W^X &= \rho_{SX} W^1 + \sqrt{1 - \rho_{SX}^2} W^2, \\ W^Y &= \rho_{SY} W^1 + \chi \sqrt{1 - \rho_{SY}^2} W^2 + \sqrt{(1 - \chi^2)(1 - \rho_{SY}^2)} W^3, \end{aligned}$$

where W^1, W^2, W^3 are three independent Brownian motions and $\chi \triangleq \frac{\rho_{XY} - \rho_{SX}\rho_{SY}}{\sqrt{1 - \rho_{SX}^2} \sqrt{1 - \rho_{SY}^2}}$. Thus, the volatilities of variance $\lambda = (\lambda_1, \lambda_2, \lambda_3)$ in the general formulation (5) can be written as:

$$\begin{aligned} \lambda_1(t, u, \xi) &= \alpha_\theta \omega \xi_0^\mu \left[(1 - \theta) \rho_{SX} e^{-\kappa_X(u-t)} + \theta \rho_{SY} e^{-\kappa_Y(u-t)} \right], \\ \lambda_2(t, u, \xi) &= \alpha_\theta \omega \xi_0^\mu \left[(1 - \theta) \sqrt{1 - \rho_{SX}^2} e^{-\kappa_X(u-t)} + \theta \chi \sqrt{1 - \rho_{SY}^2} e^{-\kappa_Y(u-t)} \right], \\ \lambda_3(t, u, \xi) &= \alpha_\theta \omega \xi_0^\mu \theta \sqrt{(1 - \chi^2)(1 - \rho_{SY}^2)} e^{-\kappa_Y(u-t)}, \end{aligned}$$

or equivalently:

$$\lambda_i(t, u, \xi) = \alpha_\theta \omega \xi_0^\mu \left(\omega_{iX} e^{-\kappa_X(u-t)} + \omega_{iY} e^{-\kappa_Y(u-t)} \right),$$

where

$$\begin{aligned} (\omega_{iX})_{i=1,2,3} &\triangleq \left((1 - \theta) \rho_{SX}, (1 - \theta) \sqrt{1 - \rho_{SX}^2}, 0 \right)^\top, \\ (\omega_{iY})_{i=1,2,3} &\triangleq \left(\theta \rho_{SY}, \theta \chi \sqrt{1 - \rho_{SY}^2}, \theta \sqrt{(1 - \chi^2)(1 - \rho_{SY}^2)} \right)^\top. \end{aligned}$$

The corresponding covariances can be expressed similarly as:

$$\begin{aligned}
 C^{X\zeta} &= \int_0^T du \int_0^u dt \sqrt{\zeta_0^t} \lambda_1(t, u, \zeta_0) \\
 &= \alpha_\theta \omega \left[(1 - \theta) \rho_{SX} \int_0^T du \zeta_0^u \int_0^u dt \sqrt{\zeta_0^t} e^{-\kappa_X(u-t)} + \theta \rho_{SY} \int_0^T du \zeta_0^u \int_0^u dt \sqrt{\zeta_0^t} e^{-\kappa_Y(u-t)} \right], \\
 C^{\zeta\zeta} &= \sum_{i=1}^3 \int_0^T ds \left(\int_s^T du \lambda_i(s, u, \zeta_0) \right)^2 \\
 &= \alpha_\theta^2 \omega^2 \sum_{i=1}^3 \int_0^T ds \left(\omega_{iX} \int_s^T du \zeta_0^u e^{-\kappa_X(u-s)} + \omega_{iY} \int_s^T du \zeta_0^u e^{-\kappa_Y(u-s)} \right)^2, \\
 C^\mu &= \int_0^T ds \int_s^T du \sqrt{\zeta_0^s} \lambda_1(s, u, \zeta_0) \left(\frac{1}{2\sqrt{\zeta_0^u}} \int_u^T dt \lambda_1(u, t, \zeta_0) + \int_s^u dr \sqrt{\zeta_0^r} \partial_{\zeta_0^u} \lambda_1(r, u, \zeta) \right).
 \end{aligned}$$

Once again using Assumption 1 and the autocorrelations provided by Bergomi and Guyon [30], we obtain

$$\begin{aligned}
 C^{X\zeta} &= \alpha_\theta \omega \zeta_0^{\frac{3}{2}} T^2 (\omega_{1X} \mathcal{J}(\kappa_X T) + \omega_{1Y} \mathcal{J}(\kappa_Y T)), \\
 C^{\zeta\zeta} &= \alpha_\theta^2 \omega \zeta_0^2 T^3 (\omega_0 + \omega_X \mathcal{I}(\kappa_X T) + \omega_Y \mathcal{I}(\kappa_Y T) + \omega_{XX} \mathcal{I}(2\kappa_X T) + \omega_{YY} \mathcal{I}(2\kappa_Y T) + \omega_{XY} \mathcal{I}((\kappa_X + \kappa_Y) T)),
 \end{aligned}$$

where

$$\begin{aligned}
 \omega_0 &= \sum_{i=1}^3 \left(\frac{\omega_{iX}}{\kappa_X T} + \frac{\omega_{iY}}{\kappa_Y T} \right)^2, \quad \omega_X = -2 \sum_{i=1}^3 \frac{\omega_{iX}}{\kappa_X T} \left(\frac{\omega_{iX}}{\kappa_X T} + \frac{\omega_{iY}}{\kappa_Y T} \right), \quad \omega_Y = -2 \sum_{i=1}^3 \frac{\omega_{iY}}{\kappa_Y T} \left(\frac{\omega_{iX}}{\kappa_X T} + \frac{\omega_{iY}}{\kappa_Y T} \right), \\
 \omega_{XX} &= \sum_{i=1}^3 \frac{\omega_{iX}^2}{\kappa_X^2 T^2}, \quad \omega_{YY} = \sum_{i=1}^3 \frac{\omega_{iY}^2}{\kappa_Y^2 T^2}, \quad \omega_{XY} = 2 \sum_{i=1}^3 \frac{\omega_{iX} \omega_{iY}}{\kappa_X \kappa_Y T^2},
 \end{aligned}$$

and

$$\mathcal{I}(z) = \frac{1 - e^{-z}}{z}, \quad \mathcal{J}(z) = \frac{z - 1 + e^{-z}}{z^2}, \quad \mathcal{K}(z) = \frac{1 - e^{-z} - z e^{-z}}{z^2}, \quad \mathcal{H}(z) = \frac{\mathcal{J}(z) - \mathcal{K}(z)}{z}.$$

Similarly, we have $C^\mu = \alpha_\theta^2 \omega^2 \zeta_0^2 T^3 (C_1^\mu + C_2^\mu)$, with the coefficients

$$\begin{aligned}
 C_1^\mu &= \frac{1}{2} \omega_{1X}^2 \mathcal{H}(\kappa_X T) + \frac{1}{2} \omega_{1Y}^2 \mathcal{H}(\kappa_Y T) - \omega_{1X} \omega_{1Y} \frac{\mathcal{J}(\kappa_Y T) - \mathcal{J}(\kappa_X T)}{(\kappa_X + \kappa_Y) T}, \\
 C_2^\mu &= \omega_X'' \mathcal{J}(\kappa_X T) + \omega_Y'' \mathcal{J}(\kappa_Y T) + \omega_{XX}'' \mathcal{J}(2\kappa_X T) + \omega_{YY}'' \mathcal{J}(2\kappa_Y T) + \omega_{XY}'' \mathcal{J}((\kappa_X + \kappa_Y) T),
 \end{aligned}$$

and

$$\begin{aligned}
 \omega_X'' &= \frac{\omega_{1X}^2}{\kappa_X T} + \frac{\omega_{1X} \omega_{1Y}}{\kappa_Y T}, \quad \omega_Y'' = \frac{\omega_{1Y}^2}{\kappa_Y T} + \frac{\omega_{1X} \omega_{1Y}}{\kappa_X T}, \\
 \omega_{XX}'' &= -\frac{\omega_{1X}^2}{\kappa_X T}, \quad \omega_{YY}'' = -\frac{\omega_{1Y}^2}{\kappa_Y T}, \quad \omega_{XY}'' = -\frac{\omega_{1X} \omega_{1Y}}{\kappa_X T} - \frac{\omega_{1X} \omega_{1Y}}{\kappa_Y T}.
 \end{aligned}$$

Since $C^{X\zeta} \sim T^2 \left(C_1 \cdot \frac{\kappa_X T - 1 + e^{-\kappa_X T}}{(\kappa_X T)^2} + C_2 \cdot \frac{\kappa_Y T - 1 + e^{-\kappa_Y T}}{(\kappa_Y T)^2} \right)$ and C_1, C_2 are constants, we can derive the term structure of the ATM volatility skew as in Equation (9) with the first order in ε . \square

However, this result derived for the Bergomi model by the Bergomi-Guyon expansion [30] is inconsistent with empirical evidence; see, for example, Bayer et al. [1]. This suggests that the power-law kernel of the forward variance curve in the rBergomi model

will lead to more realistic and accurate pricing and hedging results than the exponential kernel of the forward variance curve in the Bergomi model.

2.2. Markovian Representation of the Rough Bergomi Model

The purpose of this section is to establish the infinite-dimensional affine nature and Markovianity of the rBergomi model.

Definition 3. An Ornstein-Uhlenbeck (OU) process Y_t^x is the solution of the following stochastic differential equation (SDE):

$$dY_t^x = x(a - Y_t^x)dt + \sigma dB_t, \tag{10}$$

where $x > 0$ is the mean-reversion speed, $a > 0$ is the mean-reversion level, and B_s is a standard Brownian motion. Its strong solution is explicitly given by

$$Y_t^x = Y_0 + \sigma \int_0^t e^{-x(t-s)} dB_s. \tag{11}$$

Assumption 2. In the rest of the paper, we always assume that

$$a \triangleq Y_0, \tag{12}$$

$$\sigma \triangleq \eta \sqrt{2\alpha + 1}, \tag{13}$$

where η and α come from Definition 1 of the rBergomi model (see Bayer et al. [1]).

Definition 4. Without loss of generality, we define, for $H < \frac{1}{2}$, the sigma-finite measure $\mu(dx)$ on $(0, \infty)$ as

$$\mu(dx) = \frac{dx}{x^{\frac{1}{2}+H}\Gamma(\frac{1}{2}-H)}.$$

2.2.1. Volterra-Type Integral as a Functional of a Markov Process

Theorem 3. Using Definitions 3 and 4, the Volterra-type integral $\tilde{X}_t \triangleq \int_0^t (t-s)^{H-\frac{1}{2}} dB_s$ in the rBergomi model has the Markovian representation

$$\sigma \tilde{X}_t = \int_0^\infty (Y_t^x - Y_0) \mu(dx). \tag{14}$$

Proof. The Laplace transform of the measure μ in Definition 4 is

$$\mathcal{L}(\mu)(\tau) = \int_0^\infty e^{-\tau x} \mu(dx) = \int_0^\infty \frac{e^{-\tau x} x^{-\frac{1}{2}-H}}{\Gamma(\frac{1}{2}-H)} dx = \tau^{H-\frac{1}{2}},$$

which can be recognised as the power-law kernel in the Volterra-type integral. Consequently, we have $\sigma \tilde{X}_t = \int_0^t \int_0^\infty \sigma e^{-x(t-s)} \mu(dx) dB_s$, and using Fubini's stochastic theorem, see Protter [32], we obtain $\sigma \tilde{X}_t = \int_0^\infty \int_0^t \sigma e^{-x(t-s)} dB_s \mu(dx)$. From Definition 3, where $\int_0^t \sigma e^{-x(t-s)} dB_s = Y_t^x - Y_0$, we obtain the Markovian representation given by Equation (14). \square

Theorem 4. The OU process (11) has the affine structure

$$\mathbb{E} \left[\exp \left(\int_0^\infty Y_t^x \mu(dx) \right) \mid \mathcal{F}_s \right] = \exp \left(\frac{\sigma^2}{2} \int_0^{t-s} \left(\int_0^\infty e^{-sx} \mu(dx) \right)^2 ds + \int_0^\infty Y_s^x e^{-(t-s)x} \mu(dx) \right).$$

Proof. From Fubini’s stochastic theorem, $\int_0^\infty Y_t^x \mu(dx)$ is Gaussian under the filtration \mathcal{F}_s for $0 \leq s \leq t$, with mean

$$\mathbb{E} \left[\int_0^\infty Y_t^x \mu(dx) \mid \mathcal{F}_s \right] = \int_0^\infty Y_s^x e^{-(t-s)x} \mu(dx).$$

Furthermore, using Itô’s isometry, we have the conditional variance:

$$\begin{aligned} \text{Var} \left(\int_0^\infty Y_t^x \mu(dx) \mid \mathcal{F}_s \right) &= \sigma^2 \int_s^t \left(\int_0^\infty e^{-(t-s)x} \mu(dx) \right)^2 ds \\ &= \sigma^2 \int_0^{t-s} \left(\int_0^\infty e^{-sx} \mu(dx) \right)^2 ds. \end{aligned}$$

Thus,

$$\begin{aligned} \mathbb{E} \left[\exp \left(\int_0^\infty Y_t^x \mu(dx) \right) \mid \mathcal{F}_s \right] &= \exp \left(\frac{1}{2} \text{Var} \left(\int_0^\infty Y_t^x \mu(dx) \mid \mathcal{F}_s \right) + \mathbb{E} \left[\int_0^\infty Y_t^x \mu(dx) \mid \mathcal{F}_s \right] \right) \\ &= \exp \left(\frac{\sigma^2}{2} \int_0^{t-s} \left(\int_0^\infty e^{-sx} \mu(dx) \right)^2 ds + \int_0^\infty Y_s^x e^{-(t-s)x} \mu(dx) \right). \end{aligned}$$

□

2.2.2. Quasi-Affine Structure in the rBergomi Model

From Definition 1 and Theorem 3, the rBergomi model can be rewritten in the following form:

$$\begin{cases} dX_t = -\frac{1}{2} V_t dt + \sqrt{V_t} dW_t, \\ \log \frac{V_t}{\xi_0} = \int_0^\infty (Y_t^x - Y_0) \mu(dx), \end{cases}$$

where X_t is the log stock price, ξ_0 is the initial flat forward variance curve, and W, B are two Brownian motions with correlation $d\langle W, B \rangle_t = \rho dt$ and $\rho \in [-1, 1]$. Our aim is now to write the log stock price X_t in a quasi-affine form as the first coordinate of an infinite-dimensional affine process. To do so, we introduce the following symmetric non-negative tensor:

$$L^1(\mu) \otimes_s L^1(\mu) = \left\{ y^{\otimes 2} : y \in L^1(\mu) \right\} \subset L^1(\mu)^{\otimes 2} \subset L^1(\mu^{\otimes 2}),$$

where we used the notation $y^{\otimes 2} \triangleq y \otimes y$. Let $\Pi_t = (i \otimes 1)(Y_t^x)^{\otimes 2} \in iL^1(\mu) \otimes_s L^1(\mu)$, where i is the imaginary unit ($i \times i = -1$). The relation $(\int_0^\infty Y_t^x \mu(dx))^2 = \int_0^\infty (i \otimes 1)(Y_t^x)^{\otimes 2} \mu^{\otimes 2}(dx)$ holds. Therefore, the log stock price dynamics can be written as

$$\begin{aligned} dX_t &= \sqrt{\xi_0} \cdot \left(\mathcal{E}^{\int_0^\infty \Pi_t \mu^{\otimes 2}(dx)} dW_t - \frac{1}{2} \mathcal{E}^{\int_0^\infty Y_t^x \mu(dx)} \right) \\ &= \sqrt{\xi_0} e^{\frac{\int_0^\infty \Pi_t \mu^{\otimes 2}(dx)}{4}} e^{-\frac{\eta^2}{4} t^{2\alpha+1}} dW_t - \frac{\sqrt{\xi_0}}{2} e^{\int_0^\infty Y_t^x \mu(dx)} e^{-\frac{\eta^2}{2} t^{2\alpha+1}} dt, \end{aligned}$$

where \mathcal{E} is the Doléans-Dade stochastic exponential.

Theorem 5. The process $\Pi_t = (i \otimes 1)(Y_t^x)^{\otimes 2}$ satisfies the affine structure

$$\mathbb{E} \left[e^{\int_0^\infty \Pi_t \mu^{\otimes 2}(dx)} \mid \mathcal{F}_s \right] = e^{\Phi_1 + \Phi_2}, \tag{15}$$

where

$$\Phi_1 \triangleq -\frac{1}{2} \log \left(1 - 2 \int_0^{t-s} \left(\int_0^\infty e^{-ux} \mu(dx) \right)^2 du \right), \tag{16}$$

$$\Phi_2 \triangleq \frac{\int_0^\infty \Pi_s \left(e^{-(t-s)x} \right)^{\otimes 2} \mu^{\otimes 2}(dx)}{\sigma^2 - 2\sigma^2 \int_0^{t-s} \left(\int_0^\infty e^{-ux} \mu(dx) \right)^2 du}. \tag{17}$$

Proof. From Fubini’s stochastic theorem, $\frac{\int_0^\infty Y_t^x \mu(dx)}{\sigma \sqrt{\int_0^{t-s} \left(\int_0^\infty e^{-ux} \mu(dx) \right)^2 du}}$ is Gaussian under the filtration \mathcal{F}_s for $0 \leq s \leq t$, with conditional mean

$$\mathbb{E} \left[\frac{\int_0^\infty Y_t^x \mu(dx)}{\sigma \sqrt{\int_0^{t-s} \left(\int_0^\infty e^{-ux} \mu(dx) \right)^2 du}} \middle| \mathcal{F}_s \right] = \frac{\int_0^\infty Y_s^x e^{-(t-s)x} \mu(dx)}{\sigma \sqrt{\int_0^{t-s} \left(\int_0^\infty e^{-ux} \mu(dx) \right)^2 du}}$$

and conditional variance

$$\text{Var} \left(\frac{\int_0^\infty Y_t^x \mu(dx)}{\sigma \sqrt{\int_0^{t-s} \left(\int_0^\infty e^{-ux} \mu(dx) \right)^2 du}} \middle| \mathcal{F}_s \right) = 1.$$

Then, the random variable defined as

$$\frac{\int_0^\infty \Pi_t \mu^{\otimes 2}(dx)}{\sigma^2 \int_0^{t-s} \left(\int_0^\infty e^{-ux} \mu(dx) \right)^2 du} = \left(\frac{\int_0^\infty Y_t^x \mu(dx)}{\sigma \sqrt{\int_0^{t-s} \left(\int_0^\infty e^{-ux} \mu(dx) \right)^2 du}} \right)^2$$

is a noncentral χ^2 distribution with one degree of freedom and noncentrality parameter

$$\frac{\left(\int_0^\infty Y_s^x e^{-(t-s)x} \mu(dx) \right)^2}{\sigma^2 \int_0^{t-s} \left(\int_0^\infty e^{-ux} \mu(dx) \right)^2 du} = \frac{\int_0^\infty \Pi_s \left(e^{-(t-s)x} \right)^{\otimes 2} \mu^{\otimes 2}(dx)}{\sigma^2 \int_0^{t-s} \left(\int_0^\infty e^{-ux} \mu(dx) \right)^2 du}.$$

Thus, the Formulas (16) and (17) for Φ_1 and Φ_2 follow from the characteristic function of the noncentral χ^2 distribution, which concludes the proof. \square

Corollary 1. *The rBergomi model admits an infinite-dimensional Markovian representation.*

Proof. This corollary follows from Theorem 5 which exhibits that the rBergomi model has an exponential-affine dependence on x ; hence, the model is Markovian in each dimension. \square

3. Rough Bergomi Approximation and Monte Carlo Schemes

In this Section, we first introduce the aBergomi model which is used to approximate the rBergomi model (3). After that, we will demonstrate the existence and uniqueness of the solution of this aBergomi model. We also prove that the aBergomi model is well-defined and the solution of the aBergomi model converges to that of the rBergomi model when the number of terms n in the aBergomi model goes to infinity. At the same time, we show that the aBergomi model inherits the affine structure of the Bergomi model.

3.1. Approximation of the Rough Bergomi Model by an n -Term Bergomi Model

Since the rBergomi model can be represented by

$$\begin{cases} dS_t = S_t \sqrt{V_t} dW_t, \\ \log \left\{ \frac{V_t}{\xi_0} \right\} = \int_0^\infty \sigma \int_0^t e^{-x(t-s)} dB_s \mu(dx), \end{cases}$$

and the n -term Bergomi model with the same Brownian motion in the variance process can be represented by

$$\begin{cases} dS_t = S_t \sqrt{V_t} dW_t, \\ \log \left\{ \frac{V_t}{\xi_0} \right\} = \int_0^t \left(\sum_{i=1}^n \alpha_i e^{-\kappa_i(t-s)} \right) dB_s, \end{cases} \tag{18}$$

we can view the rBergomi model as a continuous infinite-term Bergomi model under the measure $\mu(\cdot)$, in which the mean-reversion speed x has been integrated from 0 to ∞ , with respect to the Brownian motion B_s . We can therefore approximate the rBergomi model by an n -term exponential kernel $K_{\text{exp}} = \sum_{i=1}^n \alpha_i e^{-\kappa_i(t-s)}$ instead of the power kernel $K_{\text{pow}} = \sqrt{2\alpha + 1}(t-s)^\alpha$ of the Volterra process in the rBergomi model.

Following Equation (18), after approximating the exponential kernel $K(\tau) = \int_0^\infty e^{-x\tau} \mu(dx)$ by the kernel $K^n(\tau) = \sum_{i=1}^n \alpha_i^n e^{-\tau x_i^n}$, we can rewrite the aBergomi model (18) as follows:

$$\begin{cases} dS_t^n = S_t^n \sqrt{V_t^n} dW, \\ \log \left\{ \frac{V_t^n}{\xi_0} \right\} = \sum_{i=1}^n \alpha_i^n V_t^{n,i}, \\ dV_t^{n,i} = -x_i^n (a - V_t^n) dt + \sigma dB_t \quad a = Y_0, \sigma = \eta \sqrt{2\alpha + 1}, \end{cases} \tag{19}$$

where $(\alpha_i^n)_{1 \leq i \leq n}$ are positive weights, $(x_i^n)_{1 \leq i \leq n}$ are mean-reverting speeds, and $\langle W, B \rangle_t = \rho dt$, with initial conditions $S_0^n = S_0 = 1$ and $V_0^{n,i} = V_0 = 0$.

3.1.1. Existence and Uniqueness of (S^n, V^n)

We rewrite V^n in (19) as the following stochastic equation

$$\log \left(\frac{V_t^n}{\xi_0} \right) = \sigma \int_0^t K^n(t-s) dB_s. \tag{20}$$

Theorem 6. *Under the conditions of the model (19), there exists a unique, strong, non-negative solution V^n to Equation (20).*

Proof. Øksendal and Zhang [33] imply that there exists a unique, strong, non-negative solution V^n to Equation (20) under the conditions of the model (19). \square

Then, the strong existence and uniqueness of (S^n, V^n) follows, along with its Markovianity w.r.t. the spot price S^n and the factors $V^{n,i}$ for $i \in \{1, \dots, n\}$.

3.1.2. Convergence of (S^n, V^n) to (S, V)

To prove that the solution of the aBergomi model (S^n, V^n) converges to the solution of the rBergomi model (S, V) , we need to choose a suitable $K^n(\tau) = \sum_{i=1}^n \alpha_i^n e^{-x_i^n \tau}$ to approximate $K(\tau) = \tau^{H-\frac{1}{2}}$. When $n \rightarrow +\infty$, $(V^n)_{n \geq 1} \rightarrow V$ (see Carmona et al. [34], Muravlev [35], Harms and Stefanovits [20]).

Theorem 7. *There exist weights $(\alpha_i^n)_{1 \leq i \leq n} > 0$, mean reversion speeds $(x_i^n)_{1 \leq i \leq n} > 0$, and a constant C depending on H and T only such that*

$$\|K^n - K\|_{2,T} \leq Cn^{-\frac{4H}{5}},$$

where $\|\cdot\|_{2,T}$ is the $L^2([0, T], \mathbb{R})$ norm. In particular, $\|K^n - K\|_{2,T} \rightarrow 0$ when $n \rightarrow \infty$.

The proof of this theorem can be found in Appendix A.

Applying the previous computations and the Kolmogorov tightness criterion, we can get that the sequence (S^n, V^n) is tight for the uniform topology and the limit satisfies the model (19).

3.2. Affine Structure of the aBergomi Model

In this section, we detail the affine property of the aBergomi model.

Theorem 8. *The process V^n (Equation (20)) has the following affine structure*

$$\mathbb{E}[V_t^n \mid \mathcal{F}_s] = \zeta_0 \exp \left\{ \frac{\sigma^2}{2} \sum_{i=1}^n \alpha_i^n \left(\frac{1}{x_i^n} - \frac{e^{-(t-s)x_i^n}}{x_i^n} \right) + \sum_{i=1}^n V_s^{n,i} \alpha_i^n e^{-(t-s)x_i^n} \right\}.$$

Proof. Using Theorem 4, we have

$$\begin{aligned} \mathbb{E}[V_t^n \mid \mathcal{F}_s] &= \zeta_0 \exp \left\{ \frac{\sigma^2}{2} \int_0^{t-s} (K^n(s))^2 ds + \sum_{i=1}^n V_s^{n,i} \alpha_i^n e^{-(t-s)x_i^n} \right\} \\ &= \zeta_0 \exp \left\{ \frac{\sigma^2}{2} \int_0^{t-s} \left(\sum_{i=1}^n \alpha_i^n e^{-sx_i^n} \right) ds + \sum_{i=1}^n V_s^{n,i} \alpha_i^n e^{-(t-s)x_i^n} \right\} \\ &= \zeta_0 \exp \left\{ \frac{\sigma^2}{2} \sum_{i=1}^n \alpha_i^n \left(\frac{1}{x_i^n} - \frac{e^{-(t-s)x_i^n}}{x_i^n} \right) + \sum_{i=1}^n V_s^{n,i} \alpha_i^n e^{-(t-s)x_i^n} \right\}. \end{aligned}$$

Similarly, we can derive the affine structure of S^n by Theorem 5. \square

Then, we describe the so-called hybrid scheme and introduce an algorithm to approximate the rBergomi model by the aBergomi model.

3.3. Hybrid Scheme for the rBergomi Model

Recalling Equation (3), the rough Bergomi model with time horizon $T > 0$ under an equivalent martingale measure \mathbb{P} can be written as:

$$\begin{cases} dS_t = S_t \sqrt{V_t} dW_t, \\ \frac{d\zeta_s^t}{\zeta_s^t} = \eta \sqrt{2\alpha + 1} (t - s)^\alpha dB_s, \end{cases} \tag{21}$$

where W, B are two standard Brownian motions with correlation ρ . We recall from Assumption 1 that the forward variance curve ζ_0^t is flat for all $t \in [0, T]$: $\zeta_0^t = \zeta_0 > 0$. Thus, the spot variance V_t in Equation (21) is given by

$$V_t = \zeta_0 \exp \left(\eta \sqrt{2\alpha + 1} \int_0^t (t - s)^\alpha dB_s - \frac{\eta^2}{2} t^{2\alpha+1} \right).$$

To simulate the Volterra-type integral $\tilde{X} = \sqrt{2\alpha + 1} \int_0^t (t - s)^\alpha dB_s$, we apply the hybrid scheme proposed in Bennedsen et al. [21], which approximates the kernel function of the Brownian semi-stationary processes by a Wiener integral of the power function at $t = s$ and a Riemann sum elsewhere. Let $(\Omega, \mathcal{F}, (\mathcal{F}_t)_{t \in \mathbb{R}}, \mathbb{P})$ be a filtered probability space which supports a standard Brownian motion $W = (W_t)_{t \in \mathbb{R}}$. We consider a Brownian semi-stationary process (Bss):

$$\tilde{X}_t = \int_{-\infty}^t g(t - s) \sigma_s dW_s \quad t \in \mathbb{R}, \tag{22}$$

where $\sigma = (\sigma_t)_{t \in \mathbb{R}}$ is an $(\mathcal{F}_t)_{t \in \mathbb{R}}$ -predictable process which captures the stochastic volatility of \tilde{X} and $g : (0, \infty) \rightarrow [0, \infty)$ is a Borel-measurable kernel function. We assume that $\mathbb{E}[\sigma_t^2] < \infty$ for all $t \in \mathbb{R}$ and the process is covariance-stationary, namely,

$$\begin{aligned} \mathbb{E}[\sigma_s] &= \mathbb{E}[\sigma_t], \\ \text{cov}(\sigma_s, \sigma_t) &= \text{cov}(\sigma_0, \sigma_{|s-t|}), \quad s, t \in \mathbb{R}. \end{aligned}$$

These assumptions imply that \tilde{X} is covariance-stationary. However, the process \tilde{X} need not be strictly stationary.

Assumption 3. *The assumptions regarding the kernel function g are as follows:*

(A1) For some $\alpha \in (-\frac{1}{2}, \frac{1}{2}) \setminus \{0\}$,

$$g(x) = x^\alpha L_g(x), \quad x \in (0, 1],$$

where $L_g : (0, 1] \rightarrow [0, \infty)$ is continuously differentiable, slowly varying at 0 and bounded away from 0. Moreover, there exists a constant $C > 0$ such that the derivative L'_g of L_g satisfies

$$|L'_g(x)| \leq C \left(1 + \frac{1}{x}\right), \quad x \in (0, 1].$$

(A2) The function g is continuously differentiable on $(0, \infty)$, and the derivative g' is ultimately monotonic and satisfies $\int_1^\infty g'(x)^2 dx < \infty$.

(A3) For some $\beta \in (-\infty, -\frac{1}{2})$,

$$g(x) = \mathcal{O}(x^\beta), \quad x \rightarrow \infty.$$

In order to implement the hybrid scheme to the rBergomi model, we need to introduce a particular class of non-stationary processes, namely, truncated Brownian semi-stationary (tBss) processes,

$$\tilde{X}_t = \int_0^t g(t-s)\sigma_s dW_s \quad t \geq 0, \tag{23}$$

where the kernel function $g(t)$, the volatility process σ_s , and the driving Brownian motion W_s are as defined in the definition of Bss processes. \tilde{X}_t can also be seen as the truncated stochastic integral at 0 of the Bss process \tilde{X}_t . Equation (23) is integrable since $g(t)$ is differentiable on $(0, \infty)$.

Now, we can discretise Equation (23) in time. Let N be the total number of time-steps, $\Delta t = T/N$ be the time-step size, and $t_0 = 0 \leq \dots \leq t_j = j\Delta t \leq \dots \leq t_N = T$ be a time grid on the interval $[0, T]$.

According to Bennedsen et al. [21], the observations $\tilde{X}_{t_j}^N, j = 0, 1, \dots, N$ can be computed via ($\kappa = 1$ case)

$$\tilde{X}_{t_j}^N = L_g(\Delta t)\sigma_{j-1}^N W_{j-1,1}^N + \sum_{k=1}^j g(b_k^* \Delta t)\sigma_{j-k}^N \bar{W}_{j-k}^N \tag{24}$$

using the random vectors $W_j^N, j = 0, 1, \dots, N - 1$, the random variables $\sigma_j^N, j = 0, 1, \dots, N - 1$, where $b_k^* = \left(\frac{k^{\alpha+1} - (k-1)^{\alpha+1}}{\alpha+1}\right)^{\frac{1}{\alpha}}$, and the random vectors $\bar{W}_i^N \triangleq \int_{\frac{i}{N}}^{\frac{i+1}{N}} dW_s$ (see Proposition 2.8 in Bennedsen et al. [21]). To simulate the Volterra process \tilde{X} , we use:

$$\begin{cases} L_g \equiv 1, \\ g(x) \equiv x^{H-\frac{1}{2}}, \\ \sigma(\cdot) \equiv \sqrt{2\alpha + 1}. \end{cases}$$

Then,

$$\begin{aligned} W_{j-1,1}^N &= \int_{t_{j-1}}^{t_j} (t_j - s)^\alpha dW_s \approx \left(\frac{\Delta t}{2}\right)^\alpha (W_{t_j} - W_{t_{j-1}}) \\ \bar{W}_j^N &= \int_{t_j}^{t_{j+1}} dW_s = W_{t_{j+1}} - W_{t_j} \\ \sigma_j^N &= \sigma_{t_j}. \end{aligned}$$

The corresponding matrix representation takes the form of

$$\begin{bmatrix} \tilde{X}_{t_1} \\ \tilde{X}_{t_2} \\ \tilde{X}_{t_3} \\ \vdots \\ \tilde{X}_{t_N} \end{bmatrix} = \begin{bmatrix} W_{0,1} & 0 & \cdots & 0 & 0 \\ W_{1,1} & g(b_2^* \Delta t) \bar{W}_0 & \cdots & 0 & 0 \\ W_{2,1} & g(b_2^* \Delta t) \bar{W}_1 & \cdots & 0 & 0 \\ \vdots & \vdots & \ddots & \vdots & \vdots \\ W_{N-1,1} & g(b_2^* \Delta t) \bar{W}_{N-2} & \cdots & g(b_{N-1}^* \Delta t) \bar{W}_1 & g(b_N^* \Delta t) \bar{W}_0 \end{bmatrix} \begin{bmatrix} \sigma_{t_1} \\ \sigma_{t_2} \\ \sigma_{t_3} \\ \vdots \\ \sigma_{t_N} \end{bmatrix}. \tag{25}$$

In the rBergomi model, $\sigma_{t_i} = \sigma$ is a constant for $i = 1, 2, \dots, N$ defined in Equation (13). When simulating \tilde{X}_{t_i} , we need to perform a matrix multiplication, the computational complexity of which is of order $\mathcal{O}(N^2)$ when using the conventional matrix multiplication algorithm. However, multiplying a lower triangular Toeplitz matrix can be regarded as a discrete convolution which can be evaluated efficiently by fast Fourier transform. Therefore, the computational complexity can be reduced to $\mathcal{O}(N \log N)$. The algorithm to simulate the Volterra process \tilde{X} is described in Algorithm 1 below. Then, we can use a standard Euler scheme to simulate the price $(S_{t_1}, S_{t_2}, \dots, S_{t_N})$, as shown in Algorithm 2.

Algorithm 1: Volterra process \tilde{X}

```

for  $j = 0, 1, 2, \dots, N - 1$  do
  | generate random vectors  $W_{t_j}$ 
end
for  $j = 1, 2, \dots, N$  do
  |  $W_{t_{j-1},1}^N = \left(\frac{\Delta t}{2}\right)^\alpha (W_{t_j} - W_{t_{j-1}})$ 
end
for  $j = 0, 1, 2, \dots, N - 1$  do
  |  $\bar{W}_j^N = W_{t_{j+1}} - W_{t_j}$ 
end

```

Simulate \tilde{X} by the matrix multiplication (25) using the Fast Fourier Transform.

Table 1 reports the parameters used for our numerical experiments, which are the same as in Bayer et al. [1] and Bennedsen et al. [21]. Recall from the definition of α that the chosen value $\alpha = -0.43$ corresponds to the Hurst exponent $H = 0.07$. Such small values of H are indeed consistent with empirical experiments, and one can refer to the recent works Forde et al. [36] and Gerhold [37] about the behaviour of the rBergomi model for small H .

Algorithm 2: Rough Bergomi model

```

Simulate the Volterra process  $\tilde{X}$  by the hybrid scheme following Algorithm 1
for  $t = t_1, t_2, \dots, t_N$  do
  |  $V_t = \zeta_0 \exp\left(\eta \tilde{X} - \frac{\eta^2}{2} t^{2\alpha+1}\right)$ 
end
for  $t = t_1, t_2, \dots, t_N$  do
  |  $\log(S_{t+\Delta t}) \leftarrow \log(S_t) + \sqrt{V_t} \Delta W_t - \frac{1}{2} V_t \Delta t$ 
end

```

Table 1. Parameters in the rBergomi model.

ζ_0	η	α
0.026	1.9	-0.43

3.4. Markovian Scheme for the aBergomi Model

For the sake of simplicity, we start by deriving the approximation of the rBergomi model by a Bergomi model with two terms. The same approach can be used when the

number of terms is greater than two. The two-term Bergomi model (4) that we used to approximate the rBergomi model is given by

$$\begin{cases} dS_t = S_t \sqrt{V_t} dW_t, \\ d\zeta_s^t = \eta \zeta_s^t (\alpha_1 e^{-\kappa_1(t-s)} + \alpha_2 e^{-\kappa_2(t-s)}) dB_s, \end{cases} \tag{26}$$

where $s \in [0, t)$. Here, we introduce the process y_s^t defined as

$$\begin{cases} y_s^t = \alpha_1 e^{-\kappa_1(t-s)} Y_s^1 + \alpha_2 e^{-\kappa_2(t-s)} Y_s^2, \\ dY_s^1 = -\kappa_1 Y_s^1 ds + dB_s \quad Y_0^1 = 0, \\ dY_s^2 = -\kappa_2 Y_s^2 ds + dB_s \quad Y_0^2 = 0, \end{cases} \tag{27}$$

where the two parameters κ_1 and κ_2 come from the exponential kernel K_{exp} , and Y_s^1 and Y_s^2 are two OU processes. Hence, the process y_s^t can be written as a driftless Gaussian process as follows:

$$dy_s^t = \alpha_1 e^{-\kappa_1(t-s)} dB_s + \alpha_2 e^{-\kappa_2(t-s)} dB_s,$$

and its quadratic variation is given by $\langle dy^t, dy^t \rangle_s = \zeta^2(t-s) ds$ where $\zeta(u) = \sqrt{\alpha_1^2 e^{-2\kappa_1 u} + \alpha_2^2 e^{-2\kappa_2 u} + 2\alpha_1 \alpha_2 e^{-(\kappa_1 + \kappa_2)u}}$. The forward variation process ζ_s^t can be written as $d\zeta_s^t = \eta_s^t dy_s^t$. Thus, the solution of the forward variation process is $\zeta_s^t = \zeta_0 f^t(s, y_s^t)$, where $f^t(s, y) = \exp\left(\eta y - \frac{\eta^2}{2} \chi(s, t)\right)$ and

$$\begin{aligned} \chi(s, t) &= \int_{t-s}^t \zeta^2(u) du \\ &= \int_{t-s}^t \left(\alpha_1^2 e^{-2\kappa_1 u} + \alpha_2^2 e^{-2\kappa_2 u} + 2\alpha_1 \alpha_2 e^{-(\kappa_1 + \kappa_2)u} \right) du \\ &= \alpha_1^2 e^{-\kappa_1(t-s)} \frac{1 - e^{-2\kappa_1 s}}{2\kappa_1} + \alpha_2^2 e^{-\kappa_2(t-s)} \frac{1 - e^{-2\kappa_2 s}}{2\kappa_2} + 2\alpha_1 \alpha_2 e^{-(\kappa_1 + \kappa_2)(t-s)} \frac{1 - e^{-(\kappa_1 + \kappa_2)s}}{\kappa_1 + \kappa_2}. \end{aligned} \tag{28}$$

Recall that $V_t = \zeta_t^t = \zeta_0 \exp\left(\eta y_t^t - \frac{\eta^2}{2} \chi(t, t)\right)$ and $\chi(t, t) \underset{s \rightarrow t}{\simeq} t^{2\alpha+1}$ when $s \rightarrow t$ when the number of terms n is large enough.

Using the approximation by the Bergomi model, we consider the parameters $\{\alpha_i, \kappa_i\}_{(i=1,2,\dots,n)}$ in the exponential kernel $K_{\text{exp}} = \sum_{i=1}^n \alpha_i e^{-\kappa_i(t-s)}$ on $s \in [0, t)$. Note that when $s \rightarrow t$, the power kernel $K_{\text{pow}} \rightarrow \infty$ while K_{exp} is finite. To compute the approximation numerically, we need to truncate the kernel K_{exp} . To do so, we can use the `scipy.optimize` module in Python or the `nlinfit` function in MATLAB for the nonlinear regression of the parameters $\{\alpha_i, \kappa_i\}_{(i=1,2,\dots,n)}$ and the simulated price $\{S_t\}$. We exemplify the truncation of K_{exp} by letting $s \in [0, T - \Delta t]$, the truncated parameter $\theta = T - \frac{T}{N} = T - \Delta t$, and let $T = 1$.

We define the integral I_{trunc} on the truncated region $[0, \theta t)$ and apply the scaling property of Brownian motion as follows:

$$I_{\text{trunc}} = \sum_{i=1}^n \alpha_i \int_0^{\frac{\theta t}{T}} e^{-\kappa_i(t-s)} dB_s = \sum_{i=1}^n \alpha_i \sqrt{\frac{\theta}{T}} \int_0^t e^{-\kappa_i(1-\frac{\theta}{T})s} dB_s.$$

After scaling B_s , the process y_s has to remain driftless Gaussian and satisfy $y_s = \sum_{i=1}^n \alpha_i e^{-\kappa_i(1-\frac{\theta}{T})s} Y_s^i$, where $dY_s^i = \kappa_i(1 - \frac{\theta}{T}) Y_s^i ds + dB_s$, $Y_0^i = 0$. Then, the process y_s can be written as $dy_s = \sum_{i=1}^n \alpha_i e^{-\kappa_i(1-\frac{\theta}{T})s} dB_s$. Thus, the kernel in the rBergomi model on $[0, \frac{\theta}{T} t)$ can be approximated by $I_{\text{trunc}} = \sqrt{\frac{\theta}{T}} y_t$.

In view of Equations (26) and (27) and the derivations in this subsection, a simple Monte Carlo simulation scheme for the n -term aBergomi model is given by Algorithm 3.

In practice, the truncation of the rBergomi power kernel means that, as is the case for the Riemann-sum scheme of Bennedsen et al. [21], this scheme is able to capture the shape of the implied volatility smile, but not its level. A multiplication factor is used in Algorithm 3 for each time-step to correct for this phenomenon. In practice, these factors can be estimated using another calibrated scheme, or more simply, from quoted option prices.

Algorithm 3: n-term aBergomi model when $T = 1$

```

Set initial values  $y_s = \text{zeros}(M, N), Y_0^i = 0$ 
for ( $s = t_1, t_2, \dots, t_N$ ) and ( $i = 1, 2, \dots, n$ ) do
|  $Y_{s+\Delta t} \leftarrow Y_s^i + \kappa_i(1 - \theta)Y_s^i\Delta t + \Delta W_s$ 
end
for  $t = t_1, t_2, \dots, t_N$  do
|  $V_t = \zeta_0 e^{\text{multiplication factor} \cdot \sqrt{\theta}y_t - \frac{\eta^2}{2}t^{2\alpha+1}}$ 
end
Set initial values  $\log(S_t) = 0$ 
for  $t = t_1, t_2, \dots, t_N$  do
|  $\log(S_{t+\Delta t}) \leftarrow \log(S_t) + \sqrt{V_t}\Delta W_t^1 - \frac{1}{2}V_t\Delta t$ 
end

```

4. Simulation Results

In this section, we compare the simulated volatilities of the rBergomi and aBergomi models. To demonstrate the approximation’s accuracy and efficiency, we investigate the Mean Absolute Error (MAE) of simulated results for different number of terms and number of time-steps in numerical tests.

Figure 1 displays the power kernel K_{pow} in the rBergomi model and the K_{exp} kernel of the 20-term aBergomi model with $T = 1$ and $N = 100$. This figure suggests that this K_{exp} obtained by nonlinear regression is sufficiently accurate, with a MAE of 4.05806×10^{-6} .

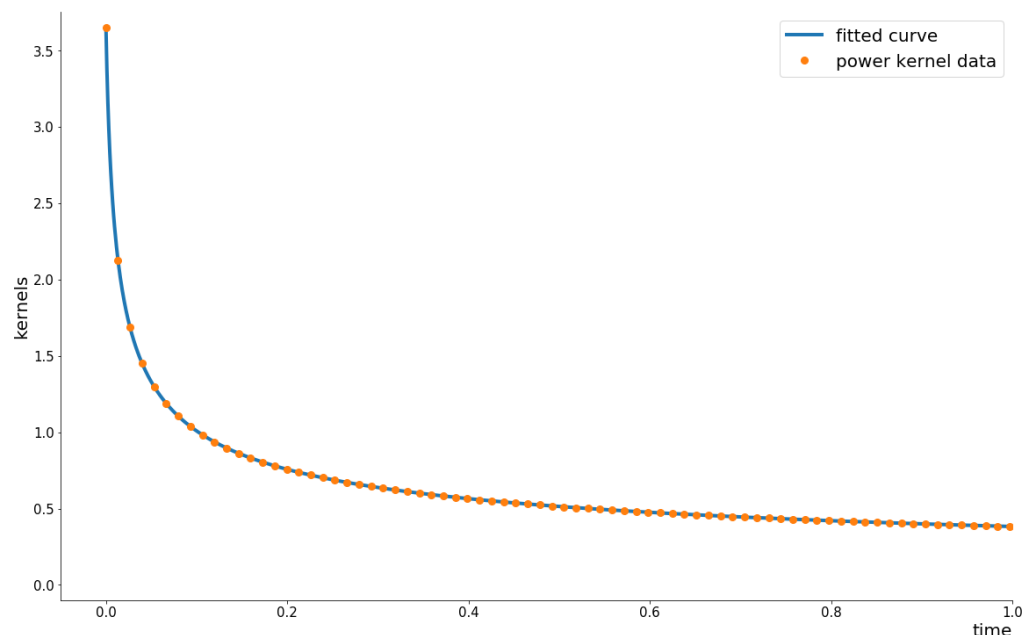


Figure 1. The power kernel K_{pow} in the rBergomi model and the exponential K_{exp} in the 20-term aBergomi model when $T = 1$ and $N = 100$.

The volatility smiles in Figure 2 are obtained by simulating the rBergomi model as described in Section 3.3, and the aBergomi model as described in Section 3.4 using the multiplication factors reported in Table 2. From Figure 2, we note that the at-the-money

calibration is better with 50 time-steps at the cost of a worse out-of-the-money calibration. Meanwhile, 100 time-steps can approximate the rBergomi model better than 50 time-steps for almost all strikes.

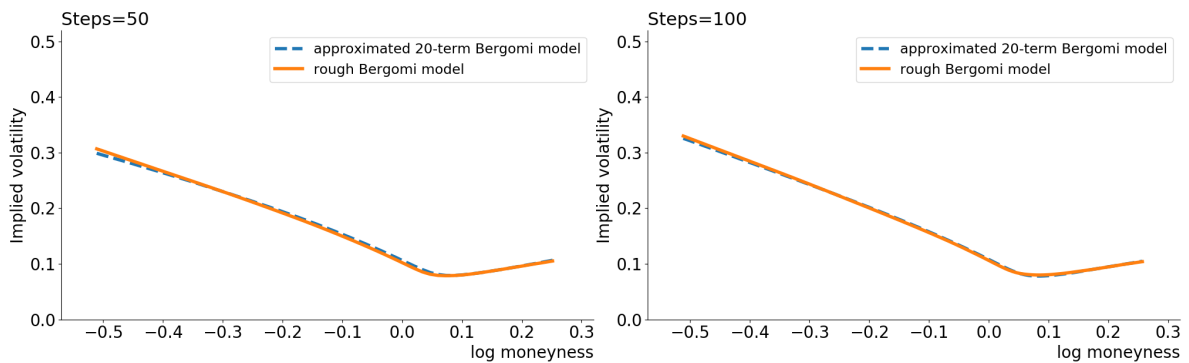


Figure 2. Volatility smiles for rBergomi and 20-term aBergomi models with $T = 1$ using 20,000 Monte Carlo paths.

Table 2. Square of multiplication factors for different steps.

Time-Steps	Square of Multiplication Factors
50	0.750324
100	0.550448
150	0.485093
200	0.450392

We compute the MAE of the implied volatility approximation with different numbers of terms in the aBergomi model and different time-steps in Figure 3, and compare the pricing speed in Table 3. As expected, the higher the number of terms in the aBergomi model, the lower the MAE for all time-steps, but the difference between the models decreases when the number of time-steps decreases. Another expected result is that the computational time increases with both the number of terms and time-steps. The number of terms and time-step combinations provide a good trade-off between speed and accuracy, such as the 20-term aBergomi model with 100 time-steps and 20,000 Monte Carlo paths.

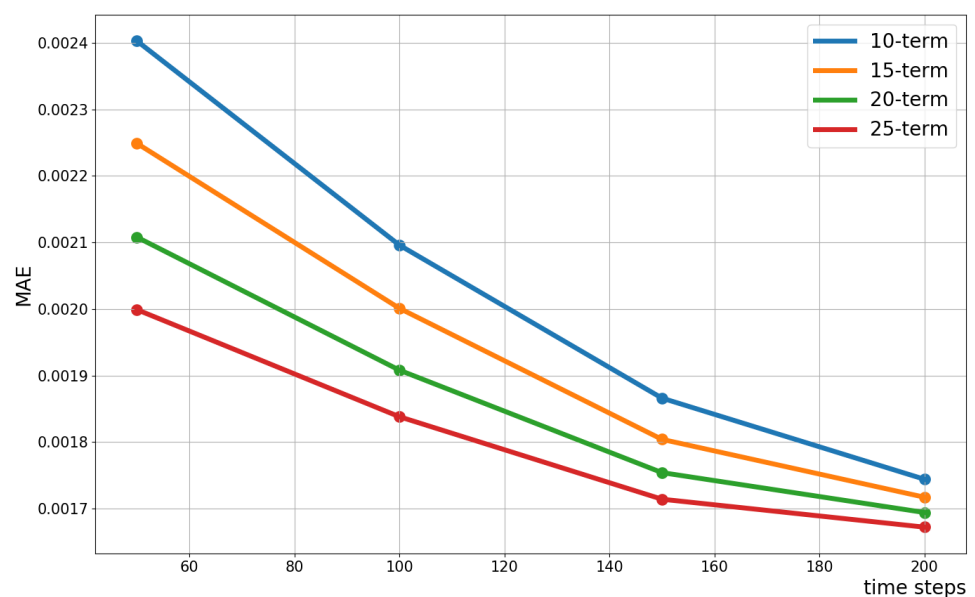


Figure 3. MAE of the implied volatility smiles of the aBergomi model with respect to the number of time-steps, for four different numbers of terms (10, 15, 20, and 25), using 20,000 Monte Carlo paths.

Table 3. Runtime (in s) of the rBergomi model and the aBergomi model for different time-steps with $T = 1$ and 20,000 Monte Carlo paths.

Time-Steps	rBergomi	10-Term aBergomi	15-Term aBergomi	20-Term aBergomi	25-Term aBergomi
50	0.4081	0.0994	0.1392	0.1721	0.2164
100	0.5001	0.2369	0.3130	0.4024	0.4543
150	0.5602	0.3650	0.4499	0.5589	0.6869
200	0.5861	0.4257	0.5908	0.7258	0.8727

5. Conclusions

In this paper, we proved the power-law behavior of the ATM volatility skew as time to maturity goes to zero of the rough Bergomi model (rBergomi), and proposed an approximate Bergomi (aBergomi) model with a finite number of forward variance terms to approximate the rBergomi model. The approximation enables the adoption of classical pricing methods, while keeping the fractional feature of the model. We theoretically prove the convergence of the aBergomi model towards the rBergomi model when the number of terms is large enough, and verify this convergence numerically. We numerically compared the fast hybrid scheme for the rBergomi model to the Euler scheme for the aBergomi model. The numerical simulation results illustrate the accuracy and efficiency of the approximation. The parameters of the aBergomi model are numerically obtained by nonlinear regression on the power-law kernel of the rBergomi model. Other alternative calibration and truncation methods are worth investigating for future research, as well as further comparisons on more complex options.

Author Contributions: Conceptualization, Q.Z. and G.L.; Formal analysis, Q.Z. and W.C.; Investigation, Q.Z.; Methodology, Q.Z. and G.L.; Software, Q.Z. and N.L.; Supervision, G.L. and W.C.; Validation, Q.Z., G.L., W.C. and N.L.; Visualization, Q.Z.; Writing—original draft, Q.Z.; Writing—review & editing, Q.Z., G.L., W.C. and N.L. All authors have read and agreed to the published version of the manuscript.

Funding: The Centre for Quantitative Finance and Investment Strategies has been supported by BNP Paribas.

Acknowledgments: The authors thank the three anonymous reviewers for their useful comments which helped us to improve the article significantly.

Conflicts of Interest: The authors declare no conflict of interest.

Appendix A

Appendix A.1. Proof of Theorem 7

This subsection is devoted to the proof of Theorem 7.

Proof. Let $(p_i^n)_{0 \leq i \leq n}$ be auxiliary mean reversion speeds such that $p_{i-1}^n \leq x_i^n \leq p_i^n$ for $i \in \{1, \dots, n\}$ and $p_0^n = 0$. Recall that $K(\tau) = \int_0^\infty e^{-x\tau} \mu(dx)$. We have

$$\begin{aligned} \|K^n - K\|_{2,T} &= \left\| \sum_{i=1}^n \alpha_i^n e^{-x_i^n \tau} - \int_0^\infty e^{-x\tau} \mu(dx) \right\|_{2,T} \\ &\leq \int_0^\infty \|e^{-x(\cdot)}\|_{2,T} \mu(dx) + \sum_{i=1}^n \left\| \alpha_i^n e^{-x_i^n(\cdot)} - \int_{p_{i-1}^n}^{p_i^n} e^{-x(\cdot)} \mu(dx) \right\|_{2,T}. \end{aligned} \tag{A1}$$

The first term on the RHS of the inequality (A1) can be estimated as below:

$$\int_{p_n^n}^\infty \|e^{-x(\cdot)}\|_{2,T} \mu(dx) = \int_{p_n^n}^\infty \sqrt{\frac{1 - e^{-2xT}}{2x}} \mu(dx) \leq \frac{(p_n^n)^{-H}}{\sqrt{2}H\Gamma\left(\frac{1}{2} - H\right)}.$$

For the second term, applying a second-order Taylor expansion of the exponential function

$$e^x = 1 + x + \frac{x^2}{2} + \int_0^x \frac{(x-u)^3}{6} du$$

for $t \in [0, T]$, choosing $\alpha_i^n = \int_{p_{i-1}^n}^{p_i^n} \mu(dx)$ and $x_i^n = \left(\frac{\int_{p_{i-1}^n}^{p_i^n} x^4 \mu(dx)}{\int_{p_{i-1}^n}^{p_i^n} \mu(dx)} \right)^{\frac{1}{4}}$, yields

$$\begin{aligned} \left| \alpha_i^n e^{-x_i^n t} - \int_{p_{i-1}^n}^{p_i^n} e^{-xt} \mu(dx) \right| &= \left| \alpha_i^n \left(1 + (-x_i^n t) + \frac{(-x_i^n t)^2}{2} \right) - \int_{p_{i-1}^n}^{p_i^n} \left(1 + (-xt) + \frac{(-xt)^2}{2} \right) \mu(dx) \right| \\ &+ \left| \alpha_i^n \left(\int_0^{x_i^n t} \frac{(x_i^n t - u)^3}{6} du \right) - \int_{p_{i-1}^n}^{p_i^n} \int_0^{xt} \frac{(xt - u)^3}{6} du \mu(dx) \right| \\ &= \int_{p_{i-1}^n}^{p_i^n} (xt - x_i^n t) + \frac{(-x_i^n t)^2 - (-xt)^2}{2} \mu(dx) \\ &\leq \frac{t^2}{2} \int_{p_{i-1}^n}^{p_i^n} (x - x_i^n)^2 \mu(dx) \end{aligned}$$

since

$$\begin{aligned} &\int_{p_{i-1}^n}^{p_i^n} \left\{ \int_0^{x_i^n t} \frac{(x_i^n t - u)^3}{6} du - \int_0^{xt} \frac{(xt - u)^3}{6} du \right\} \mu(dx) \\ &= \int_{p_{i-1}^n}^{p_i^n} \left\{ x_i^n t \int_0^1 \frac{(x_i^n t - x_i^n ts)^3}{6} ds - xt \int_0^1 \frac{(xt - xts)^3}{6} ds \right\} \mu(dx), \quad s = \frac{u}{xt} \\ &= \int_{p_{i-1}^n}^{p_i^n} \left\{ (x_i^n t)^4 \int_0^1 \frac{(1-s)^3}{6} ds - (xt)^4 \int_0^1 \frac{(1-s)^3}{6} ds \right\} \mu(dx) \\ &= \left\{ t^4 \int_0^1 \frac{(1-s)^3}{6} ds \right\} \int_{p_{i-1}^n}^{p_i^n} \left\{ (x_i^n)^4 - (x)^4 \right\} \mu(dx) \\ &= \left\{ t^4 \int_0^1 \frac{(1-s)^3}{6} ds \right\} \int_{p_{i-1}^n}^{p_i^n} \left\{ \left(\frac{\int_{p_{i-1}^n}^{p_i^n} x \mu(dx)}{\int_{p_{i-1}^n}^{p_i^n} \mu(dx)} \right)^4 - (x)^4 \right\} \mu(dx) \\ &= 0. \end{aligned}$$

Hence,

$$\sum_{i=1}^n \left\| \alpha_i^n e^{-x_i^n(\cdot)} - \int_{p_{i-1}^n}^{p_i^n} e^{-x(\cdot)} \mu(dx) \right\|_{2,T} \leq \frac{T^{\frac{5}{2}}}{2\sqrt{5}} \sum_{i=1}^n \int_{p_{i-1}^n}^{p_i^n} (x - x_i^n)^2 \mu(dx).$$

Thus, the convergence of K^n depends on the weights α_i and mean reversions x_i . Let $p_i^n = i\pi_n$ for each $i \in \{1, \dots, n\}$ and $\pi_n > 0$. We have

$$\sum_{i=1}^n \int_{p_{i-1}^n}^{p_i^n} (x - x_i^n)^2 \mu(dx) \leq \pi_n^2 \int_0^{\pi_n} \mu(dx) = \frac{\pi_n^{\frac{5}{2}-H} n^{\frac{1}{2}-H}}{\left(\frac{1}{2}-H\right)\Gamma\left(\frac{1}{2}-H\right)}$$

We can also proceed to get the explicit expressions of α_i^n and x_i^n as follows:

$$\alpha_i^n = \frac{(i\pi_n)^{\frac{1}{2}-H} - [(i-1)\pi_n]^{\frac{1}{2}-H}}{\left(\frac{1}{2}-H\right)\Gamma\left(\frac{1}{2}-H\right)}, \quad x_i^n = \frac{1-2H}{3-2H} \cdot \frac{(i\pi_n)^{\frac{3}{2}-H} - [(i-1)\pi_n]^{\frac{3}{2}-H}}{(i\pi_n)^{\frac{1}{2}-H} - [(i-1)\pi_n]^{\frac{1}{2}-H}}.$$

Since $p_n^n = n\pi_n \rightarrow \infty$, we have $\pi_n^{\frac{5}{2}-H} n^{\frac{1}{2}-H} \rightarrow 0$ as $n \rightarrow +\infty$ when $\pi_n < n^{-\frac{1}{6}}$,

$$\begin{aligned} \|K^n - K\|_{2,T} &\leq \frac{1}{\sqrt{2}H\Gamma\left(\frac{1}{2} - H\right)} \left[(p_n^n)^{-H} + \frac{T^{\frac{5}{2}}H}{\sqrt{10}\left(\frac{1}{2} - H\right)} (p_n^n)^{\frac{1}{2}-H} \pi_n^2 \right] \\ &= \frac{1}{\sqrt{2}H\Gamma\left(\frac{1}{2} - H\right)} \left[n^{-H} \pi_n^{-H} + \frac{T^{\frac{5}{2}}H}{\sqrt{10}\left(\frac{1}{2} - H\right)} n^{\frac{1}{2}-H} \pi_n^{\frac{5}{2}-H} \right] \\ &= ax^{-H} + bx^{\frac{5}{2}-H} \end{aligned} \tag{A2}$$

Let $x = \pi_n, y = ax^{-H} + bx^{\frac{5}{2}-H}$ and $y' = -aHx^{-H-1} + b\left(\frac{5}{2} - H\right)x^{\frac{3}{2}-H} = 0$; solving for x , we obtain $x^{\frac{2}{5}} = \frac{aH}{b\left(\frac{5}{2}-H\right)}$, where $a = n^{-H}$ and $b = \frac{T^{\frac{5}{2}}H}{\sqrt{10}\left(\frac{1}{2}-H\right)} n^{\frac{1}{2}-H}$

$$x = \pi_n = \left[\frac{n^{-H}H\sqrt{10}\left(\frac{1}{2} - H\right)}{T^{\frac{5}{2}}Hn^{\frac{1}{2}-H}\left(\frac{5}{2} - H\right)} \right]^{\frac{5}{2}} = \left[\frac{n^{-\frac{1}{2}}\sqrt{10}\left(\frac{1}{2} - H\right)}{T^{\frac{5}{2}}\left(\frac{5}{2} - H\right)} \right]^{\frac{5}{2}} = \frac{n^{-\frac{1}{5}}}{T} \left[\frac{\sqrt{10}\left(\frac{1}{2} - H\right)}{\left(\frac{5}{2} - H\right)} \right]^{\frac{5}{2}}$$

When $\pi_n = \frac{n^{-\frac{1}{5}}}{T} \left[\frac{\sqrt{10}\left(\frac{1}{2}-H\right)}{\left(\frac{5}{2}-H\right)} \right]^{\frac{5}{2}}$, the RHS of Equation (A2) attains its minimum and

$$\|K^n - K\|_{2,T} \leq Cn^{-\frac{4H}{5}} \text{ where } C = \frac{1}{\sqrt{2}H\Gamma\left(\frac{1}{2}-H\right)} T^H \left[\frac{\sqrt{10}\left(\frac{1}{2}-H\right)}{\frac{5}{2}-H} \right]^{-\frac{5}{2}H} \frac{5}{\frac{5}{2}-H} \text{ is a constant. } \square$$

References

1. Bayer, C.; Friz, P.; Gatheral, J. Pricing under rough volatility. *Quant. Financ.* **2016**, *16*, 887–904. [\[CrossRef\]](#)
2. Forde, M.; Zhang, H. Asymptotics for rough stochastic volatility models. *SIAM J. Financ. Math.* **1993**, *8*, 114–145. [\[CrossRef\]](#)
3. Fukasawa, M. Short-time at-the-money skew and rough fractional volatility. *Quant. Financ.* **2017**, *17*, 189–198. [\[CrossRef\]](#)
4. Gatheral, J.; Jaisson, T.; Rosenbaum, M. Volatility is rough. *Quant. Financ.* **2018**, *18*, 933–949. [\[CrossRef\]](#)
5. Jusselin, P.; Rosenbaum, M. No-arbitrage implies power-law market impact and rough volatility. *Math. Financ.* **2020**, *30*, 1309–1336. [\[CrossRef\]](#)
6. Bayer, C.; Ben Hammouda, C.; Tempone, R. Hierarchical adaptive sparse grids and quasi-Monte Carlo for option pricing under the rough Bergomi model. *Quant. Financ.* **2020**, *20*, 1457–1473. [\[CrossRef\]](#)
7. Jacquier, A.; Martini, C.; Muguruza, A. On VIX futures in the rough Bergomi model. *Quant. Financ.* **2018**, *18*, 45–61. [\[CrossRef\]](#)
8. McCrickerd, R.; Pakkanen, M. Turbocharging Monte Carlo pricing for the rough Bergomi model. *Quant. Financ.* **2018**, *18*, 1877–1886. [\[CrossRef\]](#)
9. El Euch, O.; Fukasawa, M.; Gatheral, J.; Rosenbaum, M. Short-term at-the-money asymptotics under stochastic volatility models. *SIAM J. Financ. Math.* **2019**, *10*, 491–511. [\[CrossRef\]](#)
10. Bayer, C.; Friz, P.; Gulisashvili, A.; Horvath, B.; Stemper, B. Short-time near-the-money skew in rough fractional volatility models. *Quant. Financ.* **2019**, *19*, 779–798. [\[CrossRef\]](#)
11. Friz, P.K.; Gassiat, P.; Pigato, P. Short dated smile under rough volatility: Asymptotics and numerics. *arXiv* **2020**, arXiv:2009.08814.
12. Tomas, A. Pricing of Asian Options in the Rough Bergomi Model. Ph.D Thesis, Technische Universität Wien, Wien, Austria, 2018.
13. Bayer, C.; Tempone, R.; Wolfers, S. Pricing American options by exercise rate optimization. *Quant. Financ.* **2020**, *20*, 1749–1760. [\[CrossRef\]](#)
14. Bayer, C.; Qiu, J.; Yao, Y. Pricing options under rough volatility with backward SPDEs. *arXiv* **2020**, arXiv:2008.01241.
15. Bayer, C.; Horvath, B.; Muguruza, A.; Stemper, B.; Tomas, M. On deep calibration of (rough) stochastic volatility models. *arXiv* **2019**, arXiv:1908.08806.
16. Zeron, M.; Ruiz, I. Tensoring volatility calibration Calibration of the rough Bergomi volatility model via Chebyshev Tensors. *arXiv* **2020**, arXiv:2012.07440.
17. Horvath, B.; Muguruza, A.; Tomas, M. Deep learning volatility: A deep neural network perspective on pricing and calibration in (rough) volatility models. *Quant. Financ.* **2021**, *21*, 11–27. [\[CrossRef\]](#)
18. Abi Jaber, E.; El Euch, O. Multifactor approximation of rough volatility models. *SIAM J. Financ. Math.* **2019**, *10*, 309–349. [\[CrossRef\]](#)
19. Gatheral, J.; Keller-Ressel, M. Affine forward variance models. *Financ. Stochastics* **2019**, *23*, 501–533. [\[CrossRef\]](#)

20. Harms, P.; Stefanovits, D. Affine representations of fractional processes with applications in mathematical finance. *Stoch. Process. Their Appl.* **2019**, *129*, 1185–1228. [[CrossRef](#)]
21. Bennedsen, M.; Lunde, A.; Pakkanen, M. Hybrid scheme for Brownian semistationary processes. *Financ. Stochastics* **2017**, *21*, 931–965. [[CrossRef](#)]
22. Carr, P.; Itkin, A. ADOL: Markovian approximation of a rough lognormal model. *Risk Mag.* **2019**, *32*. Available online: <https://www.risk.net/cutting-edge/banking/7209816/adol-markovian-approximation-of-a-rough-lognormal-model> (accessed on 21 February 2021).
23. Sepp, A. Log-Normal Stochastic Volatility Model: Affine Decomposition of Moment Generating Function and Pricing of Vanilla Options. 2016. Available online: <https://dx.doi.org/10.2139/ssrn.2522425> (accessed on 21 February 2021).
24. Langrené, N.; Lee, G.; Zhu, Z. Switching to nonaffine stochastic volatility: A closed-form expansion for the Inverse Gamma model. *Int. J. Theor. Appl. Financ.* **2016**, *19*, 1–37. [[CrossRef](#)]
25. Dobrić, V.; Ojeda, F. Fractional Brownian fields, duality, and martingales. In *High Dimensional Probability*; Institute of Mathematical Statistics Lecture Notes—Monograph Series; Institute of Mathematical Statistics: Beachwood, OH, USA, 2006; Volume 51, pp. 77–95.
26. Benth, F.E.; Eyjolfsson, H.; Veraart, A. Approximating Lévy semistationary processes via Fourier methods in the context of power markets. *SIAM J. Financ. Math.* **2014**, *5*, 71–98. [[CrossRef](#)]
27. Alòs, E.; León, J.; Vives, J. On the short-time behavior of the implied volatility for jump-diffusion models with stochastic volatility. *Financ. Stochastics* **2007**, *11*, 571–589. [[CrossRef](#)]
28. Bergomi, L. Smile dynamics II. *Risk Mag.* **2005**, *18*. Available online: <https://www.risk.net/derivatives/equity-derivatives/1500225/smile-dynamics-ii> (accessed on 21 February 2021). [[CrossRef](#)]
29. Bergomi, L. Smile dynamics IV. *Risk Mag.* **2009**, *22*. Available online: <https://www.risk.net/derivatives/equity-derivatives/1564129/smile-dynamics-iv> (accessed on 21 February 2021). [[CrossRef](#)]
30. Bergomi, L.; Guyon, J. Stochastic volatility’s orderly smiles. *Risk Mag.* **2012**, *25*. Available online: <https://www.risk.net/derivatives/2171452/stochastic-volatilities-orderly-smiles> (accessed on 21 February 2021).
31. Fukasawa, M. Asymptotic analysis for stochastic volatility: Martingale expansion. *Financ. Stochastics* **2011**, *15*, 635–654. [[CrossRef](#)]
32. Protter, P. Stochastic differential equations. In *Stochastic Integration and Differential Equations*; Springer: Berlin/Heidelberg, Germany, 2005; pp. 249–361.
33. Øksendal, B.; Zhang, T.-S. The stochastic Volterra equation. *Barcelona Seminar on Stochastic Analysis*; Birkhäuser: Basel, Switzerland, 1993; pp. 168–202.
34. Carmona, P.; Coutin, L.; Montseny, G. Approximation of some Gaussian processes. *Stat. Inference Stoch. Process.* **2000**, *3*, 161–171. [[CrossRef](#)]
35. Muravlev, A. Representation of a fractional Brownian motion in terms of an infinite-dimensional Ornstein-Uhlenbeck process. *Russ. Math. Surv.* **2011**, *66*, 439–441. [[CrossRef](#)]
36. Forde, M.; Fukasawa, M.; Gerhold, S.; Smith, B. *The Rough Bergomi Model as $H \rightarrow 0$ —Skew Flattening/Blow up and Non-Gaussian Rough Volatility*; King’s College London Working Paper; King’s College: London, UK, 2020.
37. Gerhold, S. Asymptotic analysis of a double integral occurring in the rough Bergomi model. *Math. Commun.* **2020**, *25*, 171–184.